

The effects of KSEA interaction on the ground-state properties of spin chains in a transverse field

Hao Fu and Ming Zhong

*Department of Physics and Institute of Theoretical Physics,
Nanjing Normal University, Nanjing 210023, P. R. China*

Peiqing Tong*

*Department of Physics and Institute of Theoretical Physics,
Nanjing Normal University, Nanjing 210023, P. R. China and
Jiangsu Key Laboratory for Numerical Simulation of Large Scale Complex Systems,
Nanjing Normal University, Nanjing 210023, P. R. China*

(Dated: October 31, 2019)

The effects of symmetric helical interaction which is called the Kaplan, Shekhtman, Entin-Wohlman, and Aharony (KSEA) interaction on the ground-state properties of three kinds of spin chains in a transverse field have been studied by means of correlation functions and chiral order parameter. We find that the anisotropic transition of XY chain in a transverse field ($XYTF$) disappears because of the KSEA interaction. For the other two chains, we find that the regions of gapless chiral phases in the parameter space induced by the DM or $XZY - YZX$ type of three-site interaction are decreased gradually with increase of the strength of KSEA interaction. When it is larger than the coefficient of DM or $XZY - YZX$ type of three-site interaction, the gapless chiral phases also disappear.

PACS numbers:

I. INTRODUCTION

In general, quantum phase transitions (QPTs) are phase transitions that the ground state of a quantum system undergoes a qualitative change by variation in a parameter of the system [1, 2]. Unlike thermodynamic phase transitions, QPTs refer to the phase transitions of the system by quantum fluctuations at absolute zero temperature. The QPTs have been extensively studied in the quantum many-body system [3–7] and strongly correlated system [8, 9]. Furthermore, the quantum entanglement [10–12] and quantum discord [13] have singularity in the region of QPTs. One of the most widely studied quantum systems is the so-called XY chain in a transverse field ($XYTF$) which has interesting QPTs belonging to two different universality classes [14]: Ising transition and anisotropic transition. They divide the phase space of $XYTF$ into three regions: x -direction ferromagnetic (FM_x), y -direction ferromagnetic (FM_y) and paramagnetic (PM) phases. Moreover, a gapless chiral phase is induced by antisymmetric Dzyaloshinskii and Moriya (DM) interaction [15]. And another system which has an analogous gapless chiral phase is the $XYTF$ with $XZY - YZX$ type of three-site interaction [16].

On the other hand, it is found that there is a symmetric helical interaction accompanying with DM interaction in the seminal paper [18]. The symmetric helical interaction is one order of magnitude smaller than the DM interaction and thus is neglected. Then, Kaplan

find this symmetric helical interaction between the local spins in the single-band Hubbard model with spin-orbit couplings (SOCs) [19]. Afterwards, Shekhtman, Entin-Wohlman, and Aharony find that the weak ferromagnetism of La_2CuO_4 can be explained by this non-negligible symmetric helical interaction [20]. Therefore, the symmetric helical interaction is called KSEA interaction for short [21–31]. By magnetization measurements, neutron diffraction, and inelastic neutron scattering experiments, KSEA interaction is present in $Ba_2CuGe_2O_7$ [22–26], Yb_4As_3 [27], $K_2V_3O_8$ [28], and La_2CuO_4 [29]. Meanwhile, the effects of KSEA interaction on the ground-state properties of spin-Peierls system [30, 31] have been studied. By regulating the topological insulator [32] and the system in the presence of Rashba spin-orbit coupling (RSOC) [33] out of equilibrium, they can synthesize and control the indirect KSEA interaction in two local spins. Therefore, it is interesting to study the effects of KSEA interaction on QPTs. In this paper, we study the effects of KSEA interaction on the ground-state properties of three kinds of chains: $XYTF$, $XYTF$ with DM interaction, $XYTF$ with the $XZY - YZX$ type of three-site interaction.

This paper is organized as follows. In Section II, we introduce the Hamiltonians of the three kinds of chains. In Section III, The phase diagrams are given by means of correlation functions and chiral order parameters. A brief conclusion is given in Section IV.

*Electronic address: pqtong@njnu.edu.cn

II. HAMILTONIANS

The Hamiltonians of the XYTF, XYTF with DM interaction and XYTF with XZY–YZX type of three-site interaction are

$$H_1^0 = - \sum_{n=1}^N \left\{ \frac{J}{2} [(1 + \gamma) \sigma_n^x \sigma_{n+1}^x + (1 - \gamma) \sigma_n^y \sigma_{n+1}^y] + h \sigma_n^z \right\},$$

$$H_2^0 = - \sum_{n=1}^N \left\{ \frac{J}{2} [(1 + \gamma) \sigma_n^x \sigma_{n+1}^x + (1 - \gamma) \sigma_n^y \sigma_{n+1}^y] + h \sigma_n^z \right\} \\ - \sum_{n=1}^N D (\sigma_n^x \sigma_{n+1}^y - \sigma_n^y \sigma_{n+1}^x)$$

and

$$H_3^0 = - \sum_{n=1}^N \left\{ \frac{J}{2} [(1 + \gamma) \sigma_n^x \sigma_{n+1}^x + (1 - \gamma) \sigma_n^y \sigma_{n+1}^y] + h \sigma_n^z \right\} \\ - \sum_{n=1}^N F (\sigma_{n-1}^x \sigma_n^z \sigma_{n+1}^y - \sigma_{n-1}^y \sigma_n^z \sigma_{n+1}^x),$$

respectively. Here, the $\sigma_n^{x,y,z}$ are the Pauli matrices, J is the nearest neighbor interactions (without loss of generality, we take $J = 1$ in this paper), h is a uniform external transverse field, $-1 \leq \gamma \leq 1$ is a parameter characterizing the degree of anisotropy of the interactions in the xy plane, D and F are the coefficient of DM and XZY–YZX type of three-site interaction, respectively.

In generally, the KSEA interaction can be written as [31]

$$H_{\text{KSEA}} = \sum_{n=1}^N \begin{pmatrix} \sigma_n^x & \sigma_n^y & \sigma_n^z \end{pmatrix} \begin{pmatrix} 0 & a_{12} & a_{13} \\ a_{12} & 0 & a_{23} \\ a_{13} & a_{23} & 0 \end{pmatrix} \begin{pmatrix} \sigma_{n+1}^x \\ \sigma_{n+1}^y \\ \sigma_{n+1}^z \end{pmatrix}.$$

Similar to reference [31], we consider a special kind of KSEA interaction: $a_{12} = K$, $a_{13} = 0$ and $a_{23} = 0$ without loss of generality. And we study the ground state properties of three kinds of chains whose Hamiltonians are

$$H_l = - \sum_{n=1}^N K (\sigma_n^x \sigma_{n+1}^y + \sigma_n^y \sigma_{n+1}^x) + H_l^0, \quad (1)$$

where $l = 1, 2$ or 3 .

By using the Jordan-Wigner, the Hamiltonians (1) can be written by spinless fermion operator, which yield

$$H_l = - \sum_{n=1}^N [A_l c_n^\dagger c_{n+1} + B_l c_n^\dagger c_{n+1}^\dagger + C_l c_{n-1}^\dagger c_{n+1} + \\ h(c_n^\dagger c_n - \frac{1}{2})] + \text{H.C.}, \quad (2)$$

where $A_1 = A_3 = 1$, $A_2 = 1 + 2Di$, $B_1 = B_2 = B_3 = \gamma - 2Ki$, $C_1 = C_2 = 0$ and $C_3 = -2Fi$, respectively. Through Fourier transforms of the fermionic operators $c_n = \sum_k c_k e^{-ikn} / \sqrt{N}$ and the Bogoliubov transformation $c_k = u_k \eta_k + v_{-k}^* \eta_k^\dagger$ (see u_k and v_k in the Appendix A), Hamiltonians (2) can be written in the momentum space and be reduced to the diagonal form [14]

$$H_l = \sum_{k=-\pi}^{\pi} \varepsilon_{l,k} (\eta_k^\dagger \eta_k - 1/2), \quad (3)$$

where

$$\varepsilon_{1,k} = \sqrt{(\cos k + h)^2 + (\gamma^2 + 4K^2) \sin^2 k}, \quad (4)$$

$$\varepsilon_{2,k} = -2D \sin k \pm \sqrt{(\cos k + h)^2 + (\gamma^2 + 4K^2) \sin^2 k} \quad (5)$$

and

$$\varepsilon_{3,k} = 2F \sin(2k) \pm \sqrt{(\cos k + h)^2 + (\gamma^2 + 4K^2) \sin^2 k}, \quad (6)$$

respectively.

III. PHASE DIAGRAMS

A. XYTF

In the light of the symmetry of Hamiltonian (1), here we consider the case of $-1 \leq \gamma \leq 1$, K , D and $F \geq 0$. In the XYTF with KESA interaction, we can use Lee–Yang zeros method [35, 36] to figure out the critical points. The zeros of $\varepsilon_{1,k}$ in the complex h plane are

$$h = -\cos(k) + i\sqrt{4K^2 + \gamma^2} \sin(k). \quad (7)$$

The diagrams of zeros are given in the Fig. 1(a) and (b) for $K = 0$ and $K \neq 0$, respectively. Without KSEA interaction ($K = 0$), the zeros are located at the line segment of $-1 \leq h \leq 1$ when $\gamma = 0$ [see the solid line in Fig. 1(a)]. It describe the phase transition point of anisotropic transition. When $\gamma \neq 0$, the zeros lie on an ellipse which intersects the real axis at $h = \pm 1$ [see the dashed line in Fig. 1(a)]. It corresponds to Ising transition. The corresponding phase diagram are showed in the Fig. 1(c). While $K \neq 0$, the zeros are located at a ellipse which intersects the real axis at $h = \pm 1$ even $\gamma = 0$ [see Fig. 1(b)]. Different from that of $K = 0$, it means that the anisotropic transition disappears because of the KSEA interaction [see Fig. 1(d)].

To understand the properties of the phases we calculated the correlation functions. The correlation functions are defined as

$$C_L^x = \langle \sigma_1^x \sigma_L^x \rangle = \langle B_1 A_2 B_2 A_3 \dots B_{L-1} A_L \rangle,$$

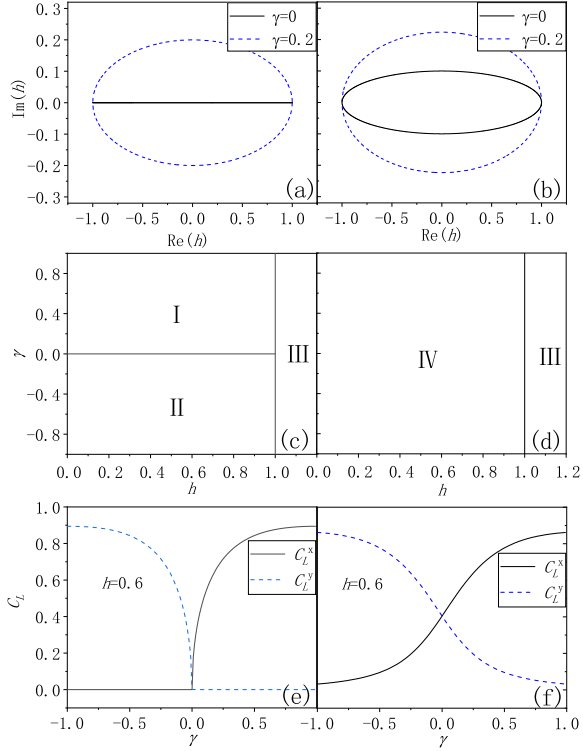


FIG. 1: (a) and (b) are the solutions of $\varepsilon(h) = 0$ in the complex h plane. (c) and (d) are the phase diagrams. (e) and (f) are the correlation functions C_L^x as a function of γ . (a), (c) and (e) $K = 0$. (b), (d) and (f) $K = 0.2$, respectively.

$$C_L^y = \langle \sigma_1^x \sigma_L^y \rangle = (-1)^{L-1} \langle A_1 B_2 A_2 B_3 \dots A_{L-1} B_L \rangle$$

with $A_n = c_n^\dagger + c_n$ and $B_n = c_n^\dagger - c_n$. The C_L^x and C_L^y can be calculated by using the Wick theorem. The basic contractions of Wick theorem are

$$\begin{aligned} G_{lm} &= \langle B_l A_m \rangle = -\langle A_m B_l \rangle \\ &= \frac{1}{N} \sum_{k=-\pi}^{\pi} \theta(\varepsilon_k) e^{-ik(l-m)} [(v_k - u_k)(u_k^* + v_k^*)] \\ &\quad + \frac{1}{N} \sum_{k=-\pi}^{\pi} \theta(-\varepsilon_k) e^{ik(l-m)} [(v_k + u_k)(u_k^* - v_k^*)], \end{aligned} \quad (8)$$

$$\begin{aligned} Q_{lm} &= \langle A_l A_m \rangle \\ &= \frac{1}{N} \sum_{k=-\pi}^{\pi} e^{-i\theta(\varepsilon_k)k(l-m)} [(v_k + u_k)(u_k^* + v_k^*)], \end{aligned} \quad (9)$$

$$\begin{aligned} P_{lm} &= \langle B_l B_m \rangle \\ &= \frac{1}{N} \sum_{k=-\pi}^{\pi} e^{-i\theta(\varepsilon_k)k(l-m)} [(v_k - u_k)(u_k^* - v_k^*)], \end{aligned} \quad (10)$$

where

$$\theta(x) = \begin{cases} 1, & x \geq 0 \\ 0, & x < 0. \end{cases} \quad (11)$$

If $K = 0$, Q_{lm} and P_{lm} always zero. The correlation functions can be simply calculated by G_{lm} (See Appendix B). However, when $K \neq 0$, the form of u_k and v_k are different from those of the XYTF without KSEA interaction so that Q_{lm} and P_{lm} nonzero anymore. We must use Pfaffian to figure out the correlation functions (See Appendix B).

The results of correlation functions are given in Fig. 1(e) and (f) with $K = 0$ and $K \neq 0$, respectively. They are not differentiable at $\gamma = 0$ when $K = 0$ (see it in Fig. 1(e)) but differentiable at $\gamma = 0$ when $K \neq 0$ (see it in Fig. 1(f)). According to the correlation functions we study the properties of the phases. In region I in Fig. 1(c), the $C_L^x \neq 0$ and $C_L^y = 0$ corresponding to FM_x phase. While the $C_L^x = 0$ and $C_L^y \neq 0$ correspond to FM_y phase in the region II in Fig. 1(c). The KSEA interaction has no effect on the properties of region III in Fig. 1(c) which corresponds to PM phase. There is a new region IV in the phase space in Fig. 1(d). In this region, the $C_L^x \neq 0$ and $C_L^y \neq 0$ correspond to a general ferromagnetic phase which is in the x -direction and y -direction (FM_{xy} phase).

B. XYTF with DM interaction

Similarly, we also use the Lee–Yang zeros method to calculate the critical points on the complex h plane for KESA interaction added on XYTF with DM interaction. The zeros in the complex h plane can be written as

$$h = -\cos(k) + \sqrt{4(D^2 - K^2) - \gamma^2} \sin(k). \quad (12)$$

There are two possible scenarios.

(i) $K < D$. The zeros with different γ in the complex h plane are given in Fig. 2(a). It is easy to check that the zeros, which lie on an ellipse, are cutting the real axis at $h = \pm 1$ in the complex h plane if $|\gamma| > 2\sqrt{D^2 - K^2}$ [see the dashed line in Fig. 2(a)]. If $|\gamma| \leq 2\sqrt{D^2 - K^2}$, from (12) we can see that the zeros lie on the real axis in the interval $|h| \leq \sqrt{4(D^2 - K^2) - \gamma^2 + 1}$. It correspond to the solid line in Fig. 2(a). From the above formula, the region of chiral phase in the parameter space decreases as K increasing.

In Fig. 2(c) and (e), phase diagram and correlation functions are shown respectively for $K < D$. In the two regions IV in Fig. 2(c), the $C_L^x \neq 0$ and $C_L^y \neq 0$ corresponding to FM_{xy} phase. The direction of the ferromagnetism is inclined to x -direction when $\gamma > 0$. For comparison, the phase diagram and correlation functions corresponding to the coefficients $K = 0$ and $D = 0.2$ are given in Fig. 2(d) and (f), respectively. In region I in Fig. 2(d), the $C_L^x \neq 0$ and $C_L^y = 0$ corresponding to FM_x phase. The $C_L^x = 0$ and $C_L^y \neq 0$ corresponding to FM_y phase in the region II in Fig. 2(d).

However, the correlation functions are not a good order parameters in the gapless chiral phase so that we calculated the chiral order parameter in the z -direction [15].

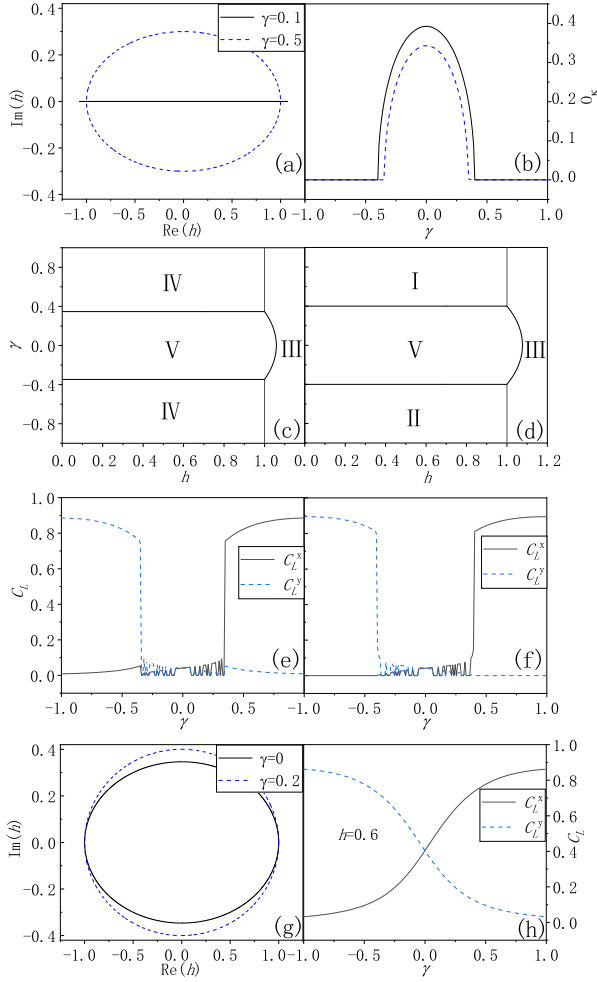


FIG. 2: (a) and (g) are the solutions of $\varepsilon(h) = 0$ in the complex h plane. (b) is the chiral order parameter as a function of γ . The solid and dashed lines correspond to the $K = 0$ and $K = 0.1$ with the same $D = 0.2$, respectively. (c) and (d) are the phase diagrams. (e), (f) and (h) are the correlation functions as a function of γ . (a), (c) and (e) $K = 0.1$, $D = 0.2$, (d) and (f) $K = 0$, $D = 0.2$. (g) and (h) $K > D = 0.2$.

$$O_\kappa = \frac{1}{N} \sum_{n=1}^N \langle \mathbf{k} \cdot \boldsymbol{\sigma}_n \times \boldsymbol{\sigma}_{n+1} \rangle, \quad (13)$$

where \mathbf{k} is the unit vector in z -direction.

We can obtain the chiral order parameter

$$O_\kappa = -\frac{4}{N} \sum_k \sin k \Theta(\varepsilon_{2,k}), \quad (14)$$

where

$$\Theta(x) = \begin{cases} 1, & x \geq 0, \\ 0, & x < 0. \end{cases} \quad (15)$$

Obviously, $O_\kappa = 0$ in regions I, II and III because ε_k are always positive. The solid and dashed lines correspond to the coefficients $K = 0$ and $K = 0.1$ with a

same $D = 0.2$, respectively (see Fig. 2(b)). Similarly, the region of chiral phase in the parameter space decreases as K increasing.

(ii) $K > D$. Equation (12) can be transformed to $h = -\cos(k) + i\sqrt{\gamma^2 - 4(D^2 - K^2)}\sin(k)$. The zeros are given in Fig. 2(g) for $\gamma = 0$ and $\gamma = 0.2$, respectively. It is found that the zeros are located at different ellipses with different γ intersecting the real axis at $h = \pm 1$. It is similar to that in the XYTF with KSEA interaction in Fig. 1(b).

In Fig. 2(h) we give the correlation functions when $K > D$. We find that the correlation functions are differentiable about $-1 \leq \gamma \leq 1$ which is similar as Fig. 1(f). The C_L^x and C_L^y are nonzero in the whole region of γ . So the phase diagram is the same as Fig. 1(d) when $K > D$.

C. XYTF with XZY - YZX type of three-site interaction

Similarly, the zeros in the complex h plane can be written as

$$h = -\cos(k) + \sqrt{16T^2 \cos^2(k) - 4K^2 - \gamma^2} \sin(k). \quad (16)$$

There are also two possible scenarios.

(i) $K < 2F$. The zeros for $K = 0.1$ and different γ respectively in the complex h plane are given in Fig. 3(a). It is easy to check that the zeros, which lie on an ellipse, are cutting the real axis at $h = \pm 1$ in the complex h plane if $\gamma > 2\sqrt{(2F)^2 - K^2}$ (see the dashed line in Fig. 2(a)). When $\gamma \leq 2\sqrt{(2F)^2 - K^2}$, the zeros are located on two line segments on the real h axis [see the solid line in Fig. 3(a)].

In Fig. 3(c) and (e), we give the phase diagram and correlation functions respectively for $K < 2F$. In the regions IV in Fig. 3(c), the $C_L^x \neq 0$ and $C_L^y \neq 0$ corresponding to FM_{xy}. We also find that the direction of the ferromagnetism is inclined to x -direction when $\gamma > 0$. For comparison, the phase diagram and correlation functions corresponding to the coefficients $K = 0$ and $F = 0.125$ are shown in Fig. 3(d) and (f), respectively. In region I in Fig. 3(d), the $C_L^x \neq 0$ and $C_L^y = 0$ corresponding to FM_x. The $C_L^x = 0$ and $C_L^y \neq 0$ corresponding to FM_y in the region II in Fig. 3(d).

To understand the properties of the phase V in Fig. 3(d), we calculate the chiral order parameters as follow

$$O_\kappa = \frac{1}{N} \sum_{n=1}^N \langle \boldsymbol{\sigma}_{n-1} \cdot (\boldsymbol{\sigma}_n \times \boldsymbol{\sigma}_{n+1}) \rangle. \quad (17)$$

After the calculation of O_κ we can obtain

$$O_\kappa = -\frac{4}{N} \sum_k [2(1 - G_{i+1,i} - G_{i,i+1})\cos(k) + (2G_{i,i} + G_{i+2,i} + G_{i,i+2})\Theta(\varepsilon_{3,k})\sin(k)], \quad (18)$$

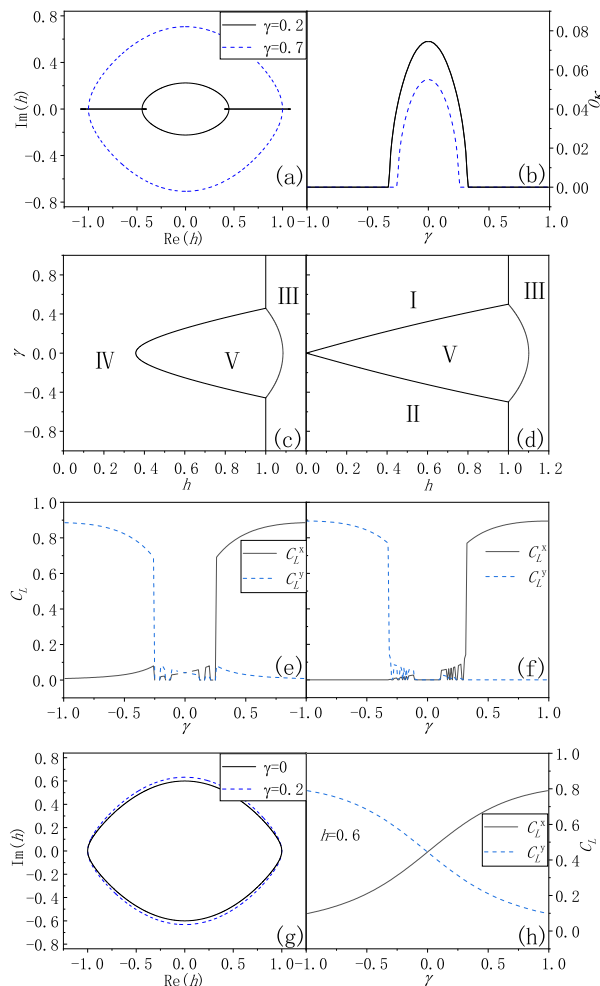


FIG. 3: (a) and (g) are the solutions of $\varepsilon(h) = 0$ in the complex h plane. (b) is the chiral order parameter as a function of γ . The solid and dashed lines correspond to the $K = 0$ and $K = 0.1$ with the same $F = 0.125$, respectively. (c) and (d) are the phase diagrams. (e), (f) and (h) are the correlation functions as a function of γ . (a), (c) and (e) $K = 0.1$, $F = 0.125$, (d) and (f) $K = 0$, $D = 0.125$. (g) and (h) $K > D = 0.125$.

where the basic contractions $\langle G_{lm} \rangle$ are the same as Equation (8) with a different form of u_k and v_k (See Appendix A). On the basis of translation invariance, all $G_{i,i+j}$ are the same with different i and the same j . The chiral order parameters in region I, II, III and IV are zero apparently and nonzero in the region V. The solid and dashed lines correspond to the coefficients $K = 0$ and $K = 0.1$ with a same $F = 0.125$, respectively (see Fig. 3(b)). Similarly, the region of chiral phase in the parameter space decreases when K increased.

(ii) $K > 2F$. Equation (16) can be transformed to $h = -\cos(k) + i\sqrt{\gamma^2 - 4[4F^2\cos^2(k) - K^2]}\sin(k)$. The diagram of zeros is given in Fig. 3(g) with $\gamma = 0$ and $\gamma = 0.2$, respectively. It is found that the zeros are located at different ellipses with different γ intersecting the real

axis at $h = \pm 1$. It is the same as the situation of XYTF with KSEA interaction in Fig. 1(b).

In Fig. 3(h) we give the correlation functions when $K > D$. We find that the correlation functions are differentiable in the interval $[-1, 1]$ which is similar as Fig. 1(f). The C_L^x and C_L^y are nonzero in the whole region of γ . So the phase diagram when $K > D$ is the same as Fig. 1(d).

IV. CONCLUSION

In summary, we have studied the effects of the KSEA interactions on the ground-state properties of the three kinds of spin chains which are XYTF, XYTF with DM interaction, XYTF with $XZY - YZX$ type of three-site interaction. In the first case, the zeros lying on the segment of real axis of the complex h plane disappear when K is nonzero. The correlation functions turn into differentiable at the point where $\gamma = 0$. So the anisotropic transition disappear because of the KSEA interaction no matter how small it is.

In the second case, if KSEA interaction is bigger than DM interaction, the system is similar to the XYTF with KSEA interaction. If KSEA interaction is smaller than DM interaction, the region of chiral phase in the parameter space decreases as K increasing. The FM_x and FM_y phases of the XYTF with DM interaction turned into a FM_{xy} phase when K is nonzero. In the FM_{xy} phase, the direction of the ferromagnetism is inclined to x -direction when γ is greater than 0.

In the third case, if KSEA interaction is bigger than twice $XZY - YZX$ type of three-site interaction, the system is similar to the XYTF with KSEA interaction too. If KSEA interaction is smaller than twice $XZY - YZX$ type of three-site interaction, the region of chiral phase in the parameter space decreases as K increasing. The FM_x and FM_y phases of the XYTF with $XZY - YZX$ type of three-site interaction turned into a FM_{xy} phase when K is nonzero. In addition, the two phases are connected when K is nonzero which is different from the previous chain. In the FM_{xy} phase, the direction of the ferromagnetism is inclined to x -direction when γ is greater than 0.

ACKNOWLEDGMENTS

The work is supported by the National Natural Science Foundation of China (Grant Nos. 11575057 and 11975126).

V. APPENDIX A

In the Bogoliubov transformations, the u_k and v_k are different from the cases without KSEA interaction. They

are

$$u_k = \frac{(2K + \gamma i) \sin k}{\sqrt{(\varepsilon_k + \cos k + h)^2 + (4K^2 + \gamma^2) \sin^2 k}},$$

$$v_k = \frac{\varepsilon_k + \cos k + h}{\sqrt{(\varepsilon_k + \cos k + h)^2 + (4K^2 + \gamma^2) \sin^2 k}},$$

for KSEA interaction added on XY chain,

$$u_k = \frac{(2K + \gamma i) \sin k}{\sqrt{(\varepsilon_k + \cos k + h + 2D \sin k)^2 + (4K^2 + \gamma^2) \sin^2 k}},$$

$$v_k = \frac{\varepsilon_k + \cos k + h + 2D \sin k}{\sqrt{(\varepsilon_k + \cos k + h + 2D \sin k)^2 + (4K^2 + \gamma^2) \sin^2 k}},$$

for KSEA interaction added on XY chain with DM interaction and

$$u_k = \frac{(2K + \gamma i) \sin k}{\sqrt{[\varepsilon_k + \cos k + h - 2F \sin(2k)]^2 + (4K^2 + \gamma^2) \sin^2 k}},$$

$$v_k = \frac{\varepsilon_k + \cos k + h - 2F \sin(2k)}{\sqrt{[\varepsilon_k + \cos k + h - 2F \sin(2k)]^2 + (4K^2 + \gamma^2) \sin^2 k}},$$

for KSEA interaction added on XY chain with $xzy - yzx$ type of three-site interaction.

VI. APPENDIX B

If $K = 0$ and all $\varepsilon_{i,k} \geq 0$, the correlation functions can be written as

$$C_L^x = \begin{vmatrix} G_{12} & G_{13} & \cdots & G_{1L} \\ \vdots & \vdots & \vdots & \vdots \\ \vdots & \vdots & \vdots & \vdots \\ G_{L-1,2} & G_{L-1,3} & \cdots & G_{L-1,L} \end{vmatrix},$$

$$C_L^y = \begin{vmatrix} G_{21} & G_{22} & \cdots & G_{2,L-1} \\ \vdots & \vdots & \vdots & \vdots \\ \vdots & \vdots & \vdots & \vdots \\ G_{L1} & G_{L2} & \cdots & G_{L,L-1} \end{vmatrix}.$$

If $K \neq 0$ or $\varepsilon_{i,k} \leq 0$ the correlation functions are [34]

$$C_L^x = (F_x)^{1/2}, \quad (19)$$

$$C_L^y = (F_y)^{1/2}, \quad (20)$$

where

$$F_x = \begin{vmatrix} 0 & G_{12} & P_{12} & G_{13} & P_{13} & \cdots & G_{1n} \\ -G_{12} & 0 & -G_{22} & Q_{23} & -G_{32} & \cdots & Q_{2n} \\ -P_{12} & G_{22} & 0 & G_{23} & P_{23} & \cdots & G_{2n} \\ \vdots & \vdots & \vdots & \vdots & \vdots & \vdots & \vdots \\ -G_{1n} & -Q_{2n} & \cdots & \cdots & \cdots & \cdots & 0 \end{vmatrix},$$

$$F_y = \begin{vmatrix} 0 & -G_{21} & Q_{12} & -G_{31} & Q_{13} & \cdots & -G_{n1} \\ G_{21} & 0 & G_{22} & P_{23} & G_{23} & \cdots & P_{2n} \\ -Q_{12} & -G_{22} & 0 & -G_{32} & Q_{23} & \cdots & -G_{n2} \\ \vdots & \vdots & \vdots & \vdots & \vdots & \vdots & \vdots \\ G_{n1} & -P_{2n} & \cdots & \cdots & \cdots & \cdots & 0 \end{vmatrix}.$$

- [1] S Sachdev, *Quantum Phase Transitions* (Cambridge: Cambridge University Press) (1999)
- [2] M. Takahashi, *Thermodynamics of One – dimensional Solvable4 models*, Cambridge University Press, Cambridge, (1999)
- [3] S. Katsura, Phys. Rev. 127 1508 (1962)
- [4] E. R. Smith, J. Phys. C 3 1419 (1970)
- [5] J. H. H. Perk, H.W. Capel, M.J. Zailhof, Th.J. Siskens, Physica A 81 319 (1975)
- [6] H. Nishimori, Phys. Lett. A 100 239 (1984)
- [7] O. Derzhko, J. Richter, Phys. Rev. B 55 14,298 (1997)
- [8] G. I. Japaridze, R. M. Noack, D. Baeriswyl and L. Tincani, Phys. Rev. B 76 115118 (2007)
- [9] C.-B. Duan, W.-Z. Zhong, J. Phys.: Condens. Matter 22, 345601 (2010)
- [10] C.-C. Liu, J.-D. Shi, Z.-Y. Ding, L. Ye. Quantum Inf. Process. 15, 3209-3221 (2016)
- [11] K. G. Wilson, Rev. Mod. Phys. 47, 773 (1975)
- [12] A. Langari, Phys. Rev. B, 69, 100402 (2004)
- [13] T. Werlang, C. Trippe, G. A. P. Ribeiro, Gustavo Rigolin. Phys. Rev. Lett. 105, 095702 (2010)
- [14] Lieb E, Schultz T and Mattis D Ann. Phys. NY 16 407 (1961)
- [15] M. Zhong, H. Xu, X.-X. Liu, and P.-Q. Tong, Chin. Phys. B 22, 090313 (2013)
- [16] X.-X. Liu, M. Zhong, H. Xu and P.-Q. Tong, J. Stat. Mech. P01003 (2012)
- [17] I. Dzyaloshinskii, J. Phys. Chem. Solids 4, 241 (1958)
- [18] T. Moriya, Phys. Rev. 120, 91 (1960); Phys. Rev. Lett. 4, 228 (1960)
- [19] T. A. Kaplan, Z. Phys. B 49, 313 (1983).
- [20] L. Shekhtman, O. Entin-Wohlman, A. Aharony, Phys. Rev. Lett. 69, 836 (1992)
- [21] J. Chovan, M. Marder, N. Papanicolaou, Phys. Rev. B

- 88, 064421 (2013)
- [22] A. Zheludev, S. Maslov, I. Tsukada et al., Phys. Rev. Lett. 81, 5410 (1998)
- [23] A. Zheludev, S. Maslov, G. Shirane et al., Phys. Rev. B 59, 11432 (1999)
- [24] I. Tsukada, J. Takeya, T. Masuda, K. Uchinokura, Phys. Rev. B 62, R6061 (2000)
- [25] S. Mühlbauer, S. Gvasaliya, E. Ressouche et al., Phys. Rev. B 86, 024417 (2012)
- [26] S. Mühlbauer, G. Brandl, M. Månsson, M. Garst, Phys. Rev. B 96, 134409 (2017)
- [27] H. Shiba, K. Ueda, and O. Sakai, J. Phys. Soc. Jpn. 69, 1493 (2000)
- [28] M. D. Lumsden, B. C. Sales, D. Mandrus et al., Phys. Rev. Lett. 86, 159 (2001)
- [29] I. Tsukada, X. F. Sun, Seiki Komiya et al., Phys. Rev. B 67, 224401 (2003)
- [30] L. Shu, Y.-G. Chen, H. Chen, Acta Phys. Sin. 51, 902 (2002)
- [31] Z.-G. Wang, Y.-G. Chen, H. Chen, H.-L. Liu, and Y.-L. Shi, Acta Phys. Sin. 54, 2329 (2005)
- [32] P. D. Kurilovich, V. D. Kurilovich, and I. S. Burmistrov, Phys. Rev. B 94, 155408 (2016)
- [33] T.-T. Liu, J. Ren, and P.-Q. Tong, Phys. Rev. B 98, 184426 (2018)
- [34] J. Stolze, V. S. Viswanath and G. Z. Muller, Phys. B 89, 45 (1992)
- [35] C.-N. Yang, T.-D. Lee, Phys. Rev. 87 404 (1952)
T.-D. Lee, C.-N. Yang, Phys. Rev. 87 410 (1952)
- [36] P.-Q. Tong, X.-X. Liu, Phys. Rev. Lett. 97 017201 (2006)